The oxidative potential of PM_{10} from coal, briquettes and wood charcoal burnt in an experimental domestic stove

Longyi Shao [1*], Cong Hou [1], Chunmei Geng [2], Junxia Liu [3], Ying Hu[1], Jing Wang [2], Tim Jones [4], Chengmei Zhao[1], Kelly BéruBé [5]

1. State Key Laboratory of Coal Resources and Safe Mining, School of Geosciences and Survey Engineering, China University of Mining and Technology (Beijing), Beijing 100083, China;

2. Chinese Research Academy of Environmental Sciences, Beijing 100012, China;

3. China Association of Resource Comprehensive Utilization, Beijing 100082, China.

4. School of Earth and Ocean Sciences, Cardiff University, Park Place, Cardiff, UK

5. School of Biosciences, Cardiff University, Museum Avenue, Cardiff, UK

** Email: ShaoL@cumtb.edu.cn*

Highlights:

1. Burning raw powdered coal emits more PM than burning honeycomb briquette.
2. The PM_{10} emitted by burning honeycomb briquettes had a higher oxidative potential.
3. The water-soluble heavy metals in PM_{10} were associated with high oxidative potential.
4. Burning raw powdered coal had a higher health risk than burning honeycomb briquette.

Abstract: Coal contains many potentially harmful trace elements. Coal combustion in unvented stoves, which is common in most parts of rural China, can release harmful emissions into the air that when inhaled cause health issues. However, few studies have dealt specifically with the toxicological mechanisms of the particulate matter (PM) released by coal and other solid fuel combustion. In this paper, PM_{10} particles that were generated during laboratory stove combustion of raw powdered coal, clay-mixed honeycomb briquettes, and wood charcoal were analysed for morphology, trace element compositions, and toxicity as represented by oxidative DNA damage. The analyses included Field Emission Scanning Electron Microscopy (FESEM),

Inductively Coupled Plasma Mass Spectrometry (ICP-MS) and Plasmid Scission Assay (PSA). Gravimetric analysis indicated that the equivalent mass concentration of PM_{10} emitted by burning raw powdered coal was higher than that derived by burning honeycomb coal. FESEM observation revealed that the coal burning-derived PM_{10} particles were mainly soot aggregates. The PSA results showed that the PM_{10} emitted by burning honeycomb briquettes had a higher oxidative capacity than that from burning raw powdered coal and wood charcoal. It is also demonstrated that the oxidative capacity of the whole particle suspensions were similar to those of the water soluble fractions; indicating that the DNA damage induced by coal burning-derived PM_{10} were mainly a result of the water-soluble fraction. An ICP-MS analysis revealed that the amount of total analysed water-soluble elements in the PM_{10} emitted by burning honeycomb briquettes was higher than that in PM produced by burning raw powdered coal, and both were higher than PM from burning wood charcoal. The total analysed water-soluble elements in these coal burning-derived PM_{10} samples had a significantly positive correlation with the level of DNA damage; indicating that the oxidative capacity of the coal burning-derived PM_{10} was mainly sourced from the water soluble elements. The water-soluble As, Cd, Ge, Mn, Ni, Pb, Sb, Se, Tl, and Zn showed the highest correlation with the oxidative potential, implying that these elements in their water soluble states were the primary responsible factor for the plasmid DNA damage. The exposure risk was further assessed using the particle mass concentrations multiplied by the percent of DNA damage under the dose of 500 μg ml^{-1}. The results revealed that the exposure risk of burning raw powdered coal was much higher than that of burning honeycomb coal.

Key words: plasmid scission assay; inductively coupled plasma mass spectrometry (ICP-MS); coal burning-derived PM_{10}; oxidative potential; water-soluble elements; exposure risk

1. Introduction

Emissions from coal combustion represent an important source of gaseous and particulate pollutants in the atmosphere, and these pollutants can have a significant impact on atmospheric chemistry, climate change, and human health (Dockery et al., 1993; Levine et al., 1995; Samet

et al., 2000; Andreae and Merlet, 2001; Kan et al., 2007, 2012; Jones et al., 2009). Epidemiological investigations have demonstrated the association between exposure to particulate matter (PM) and an increased incidence of mortality and morbidity from lung cancer and cardiovascular diseases (Crabbe, et al., 2012; Xu et al., 2003; Hoek et al., 2013; Kheirbek, et al., 2013; Shao et al., 2013). Recently, a literature review by Pui et al. (2013) demonstrated that the components in $PM_{2.5}$ from coal combustion and from vehicle emissions are the dominant contributors to regional haze in China; they also demonstrated that short-term exposure to $PM_{2.5}$ is strongly associated with an increased risk of morbidity and mortality from cardiovascular and respiratory diseases in China. Smoky coal used domestically indoors in China is a known human carcinogen, and outdoor air containing coal-burning emissions is also considered as a potential human lung carcinogen, (Loomis et al., 2013).

China is the largest coal producer and consumer in the world. In 2013, China produced 3.7 billion tons of coal and consumed approximately 3.61 billion tons of coal (China Statistical Yearbook, 2013), which was equal to approximately 68% of the primary energy consumed in China. Residential coal stoves are commonly used for cooking and heating, especially in the winter. Approximately 25% of the coal production in China is high-sulphur coal, with a sulphur content exceeding 2%, and the burning of these high-sulphur coals releases SO_2, together with NO_2 and PM_{10} into the atmosphere, resulting in atmospheric pollution (Luo, 2008; Chen et al., 2009). Furthermore, coal contains many potentially harmful trace elements that may be minimal on average, but can be enriched as a result of special geologic conditions (Bogdanovic et al., 1995; Xu et al., 2003; Dai et al., 2003; Shao et al., 2003; Tang et al., 2004; Ren et al., 2006; Li et al., 2006). During the combustion, processing, and utilization of coal, these trace elements can be released into the air, causing harm to the environment and human health (Neas, 2000). Although we know that coal combustion can release harmful substances into the air, the toxicological mechanisms of the inhaled PM released by coal-combustion is still not clear. Although toxic metals are found to be associated with some types of coals (Tang et al., 2004; Ren et al., 2006), it is still unclear which elements emitted during coal combustion are of most concern in terms of their toxicity.

A number of studies have shown that atmospheric PM_{10}, in which coal-burning particles

dominate, is implicated in increased morbidity and mortality and can cause asthma, respiratory disease, and respiratory inflammation; it can even involve the cardiovascular system, nervous system, immune system and may eventually cause cancer (Zhang et al., 2003; Ostro et al. 2006; Lin et al. 2007; Loomis et al., 2013). Although the biological mechanisms underlying the induction of lung cancer by PM_{10} have been examined extensively (Straif et al., 2006; Benbrahim-Tallaa et al., 2012; Loomis et al., 2013), the role played in these adverse health effects by coal burning-derived PM_{10} remain unclear. A widely accepted hypothesis is that oxidative damage originates from the bioreactive surface of airborne particles (Donaldson et al., 1996; Li et al., 1997; Shao et al., 2007); the bioavailable transition metals on the surface of airborne particles could activate oxidants that could damage DNA (Costa et al., 1997; Greenwell et al., 2003; DiStefano et al., 2009; Sánchez-Pérez et al., 2009; Vidrio et al., 2009; Zhong et al., 2010). Many other studies have also shown that soluble metal components produce Reactive Oxygen Species (ROS), which can induce oxidative stress and inflammation in the lungs and respiratory tract (See et al., 2007; Distefano et al., 2009; Vidrio et al., 2009; Zhong et al., 2010). The USA Environmental Protection Agency (USEPA) defines Zn and Pb as toxic elements, and Zn is regarded as a bioreactive element (Adamson et al., 2000). Other studies have also indicated that Zn is likely to be a major element responsible for particle-induced plasmid DNA damage (Greenwell et al., 2003; Shao et al., 2006, 2007; Lu et al., 2006). Lan and co-workers (2004) demonstrated oxidative damage-related genes (e.g. *AKR1C3* and *OGG1)* modulated risks for lung cancer due to exposure to PAH-rich coal combustion emissions. Their human molecular epidemiology study took place in Xuan Wei County, China, which had the highest lung cancer rates in China. It was demonstrated that PAHs were activated to genotoxic intermediates to produce PAH metabolites that form DNA adducts or reactive oxygen species (ROS) leading to oxidative DNA damage, such as 8-hydroxy-2′-deoxyguanosine (8-oxo-dG).

Currently, many methods are employed in the toxicological study of atmospheric particles; such as irrigation, the Ames test method, micronucleus experiments, chromosome aberration tests, and the comet assay. However, most of these are only qualitative techniques. In recent years, a plasmid DNA scission assay has been developed to study the toxicity of atmospheric

particulates (Li et al., 1997; Whittaker, 2003; Shao et al., 2007； Chuang et al., 2011, 2013); it is a simple, rapid, high-sensitivity technique to detect DNA damage and allows for the toxicity of particles to be quantified. This method has been proved to be effective in characterizing the oxidative capacity of coal burning-derived particles (Wang et al., 2014). Inductively Coupled Plasma Mass Spectrometry (ICP-MS) can be used to measure the levels of the water-soluble trace elements responsible for the particle-induced DNA damages (Shao et al., 2006).

This paper evaluates the oxidative damage to plasmid DNA by PM_{10} generated by laboratory-stove combustion of different types of Chinese coal. The water-soluble trace elements of PM_{10} were examined using ICP-MS. The aim of this paper was to assess the toxicity of coal burning-derived PM_{10} and the relationship between the particle-induced oxidative potential and the metal compositions of these coal burning-derived PM_{10}.

2. Sampling and experiments

2.1 Combustion system and sample collection

The coals that were used in these experiments were collected from a number of coal mining areas, including Zhijin in Guizhou Province (ZJ), Datong in Shanxi Province (DT), Dongsheng in the Inner Mongolia Autonomous Region (DS), Yinchuan in the Ningxia Hui Autonomous Region (YC), and Jingxi (western Beijing mountain) in Beijing (JX). Raw, loose, powdered coals were prepared from ZJ, DT, DS, YC, and JX, and the clay-mixed honeycomb briquettes were prepared from ZJ and DT by a combination of 80% raw powdered coals and 20% clay. Wood charcoal was used as a comparison in the experiments. Information about the proximate and ultimate analyses of raw powdered coals used in this study is given in Table 1.

We used a laboratory-made combustion system to conduct the burning experiments, which were carried out at the Laboratory of the Chinese Research Academy of Environmental Sciences (Geng et al., 2012). The system was composed of a combustion stove with smoke dilution tunnels and smoke chambers. The coal-stove, which is used widely for domestic cooking and heating in China, was purchased from the grocery market. It has a metallic outer cover and thermal-insulated ceramic liner. The cylindrical inner volume is 0.01 m^3. The dilution tunnel consisted of two main parts made of stainless steel, including an orthogonal

pipe and a cylindrical tunnel, and an attached suction fan. The orthogonal pipe with a length of 1 m and a radius of 20 cm was connected to the stove for flue gas introduction and first-step dilution with filtered air. At the end of the orthogonal pipe, a horizontal cylindrical tunnel with a length of 4 m and a radius of 40 cm was connected for second-step dilution. At the end of the tunnel, there were several outlets for suction fans and sampling. The flow rate of the suction fan was controlled by a Venturic tube and was fixed at 5800 L/min. The residence time of flue gas in the dilution tunnel was 5.5 second. After second-step dilution, the temperature of diluted flue gas decreased to 30°C. The smoke chamber connected to the horizontal cylindrical tunnel was used for real-time measurement of gaseous and particulate pollutant during the combustion experiments. Our PM_{10} sampler was connected to this smoke chamber. During the experiments, the flow rate of the diluted flue gas into smoke chamber was fixed at 100 L/min.

Coal samples were ignited in the stove using pre-weighed wood charcoal (0.5 kg). To minimise the influence of charcoal burning emissions, the coal samples (1.0 kg for each experiment) were put into the stove until smoking from charcoal combustion stopped. Sampling started when the raw coal samples were put into the stove and ended when the combustion was complete, and the whole process lasted for approximately one hour. The schematic diagram showing this combustion system is shown in Figure 1.

A medium-volume particle sampler (Dickel-80, Beijing Geological Instrument Dickel Cooperation limited, China) and a Minivol^{TM} particle sampler (Air Metric, U.S.A), which were connected to the dynamic smoke chamber, were used to collect the particulate matter. Particles with an aerodynamic diameter of 10 μm or less were collected. Quartz fibre filters (diameter 90 mm) were used in the Dickel-80 sampler (flow rate 78 L/min), and were used for the plasmid scission assay and ICP-MS experiments. Polycarbonate filters (diameter 47 mm) were used in the Minivol sampler (the flow rate was 5 L/min), and were used for the Field Emission Scanning Electron Microscopy (FESEM).

2.2 FESEM analysis

A Field Emission Scanning Electron Microscope (FESEM) (JSM-6700F) was used to investigate the morphology of the particles. Approximately one eighth of each polycarbonate

filter was cut and then mounted onto a copper washer using epoxy resin. The specimen was gold-coated to a thickness of 20 nm. Secondary electron images were obtained to analyse the morphology of the burning-derived PM_{10} particles.

2.3 Plasmid Scission Assay

The plasmid scission assay is an *in-vitro* method for assessing and comparing the oxidative potential of inhalable particles (Greenwell et al., 2003; Reche et al., 2012; Xiao et al., 2013; Chuang et al., 2013; Sun et al., 2014). The assay is based on the principle that any free radicals associated with particle surfaces can damage the supercoiled DNA by "nicking" the strands. This damage initially causes the DNA to unwind from being supercoiled into a relaxed coil. Further damage results in linearization followed by complete fragmentation. This change in structure alters the electrophoretic mobility of the DNA, thereby allowing for separation and quantification on an agarose gel.

A detailed experimental procedure has been described in Merolla and Richards (2005), Shao *et al*. (2006), Reche *et al*. (2012) and Chuang et al. (2013). The PM_{10} samples, together with a procedural blank filter, were incubated in HPLC-grade water. The incubations were gently agitated in a vortex mixer (Scientific Industries, Vortex Genie 2) for 20 h at room temperature to ensure the maximum mixing of the PM_{10} sample in water and to avoid sedimentation. At this stage after incubation each sample was separated into two parts; one part was taken to directly represent the intact whole-particle suspension, and another part was used to prepare the water-soluble fraction. The water-soluble fraction of PM_{10} sample was obtained by spinning the intact whole-particle suspension in a centrifuge (D37520, Germany) at 13000r/min for 80 minutes. At the end of this centrifuging, the supernatant was collected using a pipette; this supernatant represented the soluble fraction of the PM_{10} samples. The plasmid scission assay was used for both the intact whole-particle suspension and the centrifuged water-soluble fraction of the PM_{10} sample. Each of them was sequentially diluted into five particle dosages; 25, 50, 100, 300, and 500 $\mu g\ ml^{-1}$ respectively. All of the dose-scaled incubations were calibrated into a final volume of 20 µl, each containing 200 ng of φX174-RF DNA (Promega Corporation, USA). The prepared dose-scaled incubations were gently agitated in a vortex mixer for another 6 h to ensure the maximum mixing of the PM_{10} sample with DNA. At this

stage, bromophenol blue dye (3.5 μl) was added to each dose-scaled sample before injecting the sample into the gel which is composed of 0.6% agarose and 0.25% ethidium bromide. Then the gel carrying the injected samples was placed in a 30 V electrophoretic voltage for 16 h at room temperature in a 1% tris-borate-EDTA (TBE) buffer. The electrophoresis gels were photographed and a densitometric analysis was performed using the Genetools program (TRANSILLUMINATOR 2020D). A semi-quantitative protocol was established that measured the relative proportion of damaged DNA (relaxed and linearized) in each lane of the gel, and was expressed as a percentage of the total DNA in each lane. Two replicates of each lane were quantified in this way, and the means were recorded for each particle dosages. Subtracting the damage caused by the negative control (HPLC-grade water), the DNA damage that was induced by the airborne particles at different dosages was calculated.

To guarantee the accuracy of the experiment result, we analysed one procedural blank quartz fibre filter. The oxidative damage to plasmid DNA induced by the blank quartz fibre filter was below 10%, so it was considered that the quartz filter does not have a significant influence on the experimental results. In addition, the water-soluble fraction obtained after centrifuging will have had any broken quartz filter shards removed, thus avoiding any extra oxidative damage.

2.4 ICP-MS analysis

This study used a high-resolution Inductively Coupled Plasma Mass Spectrometer (model number: ELEMENT; Manufacturer: Finnigan-MAT company) for the analysis of trace elements from coal burning-derived PM_{10} with a detection limit of 1ppt~1ppb (10^{-12}~10^{-9}). The experiments were carried out at a laboratory in the Beijing Research Institute of Uranium Geology. The procedure used was based on Shao et al. (2013). Water-soluble trace elements were obtained by directly analysing the water-soluble fractions of the PM_{10} samples that were previously processed by centrifugation before the plasmid scission assay. The results were reported as a concentration of the element in its soluble form in the intact PM_{10} sample, which were expressed in ppm by weight.

3 Results

3.1 Mass concentration and particle morphology of the coal burning-derived PM_{10}

In order to investigate the relative amounts of PM_{10} emitted by burning different fuels, the equivalent (equal amount of fuel, equal time of combustion, and equal combustion conditions) mass concentration of the coal burning-derived PM_{10} were estimated by combining the sampling air volume and the loaded PM_{10} mass in filters. The equivalent mass concentration can be calculated by following formula:

$$MC(ug/m^3) = \frac{M_2 - M_1}{V}$$

In this formula, MC represented equivalent mass concentration of the coal burning-derived PM_{10} ($\mu g/m^3$), M_1 represented the mass of the quartz fibre filters before sampling (μg), M_2 represented the mass of the quartz fibre filters loaded with particles after sampling (μg), V represented the sampling volume (m^3), which was the value of sampling time multiplied by the flow rate of the sampler.

Table 2 showed the mass concentrations of the PM_{10} emitted by burning different coals. The mass concentration of the coal burning-derived PM_{10} varied greatly, ranging from 689 $\mu g/m^3$ for the DT honeycomb briquette to 10694 $\mu g/m^3$ for the DS raw powdered coal. The mass concentrations of the PM_{10} emitted by burning honeycomb briquette were from 689 $\mu g/m^3$ to 1282 $\mu g/m^3$, and averaged 986 $\mu g/m^3$. The mass concentrations of the PM_{10} emitted by raw powdered coal were from 1436 $\mu g/m^3$ to 10694 $\mu g/m^3$, and averaged 5251 $\mu g/m^3$. This result demonstrated that the mass concentration of PM_{10} emitted by burning raw powdered coal was higher than that by burning honeycomb briquette.

FESEM observation revealed that the morphology types of coal burning-derived particles were almost all soot aggregates, which consisted of many carbon spheres. Figure 2 demonstrates that the number density per unit area in the images of the PM_{10} emitted by burning honeycomb briquette was relatively small, while number density per unit area in the images of the PM_{10} emitted by burning raw powdered coal was much denser. This reconfirmed that burning raw powdered coal would generate more particles than burning honeycomb briquettes.

3.2 Oxidative potential of PM_{10} generated from burning different types of coal

The oxidative potential of the PM_{10} generated by burning honeycomb briquettes, the raw powdered coals, and the wood charcoal were examined with a plasmid scission assay. A total of 8 types of PM_{10} samples were used in this study and represented emissions from burning raw powdered coals from ZJ, DT, DS, YC, and JX, the clay-mixed honeycomb briquettes from ZJ and DT, and wood charcoal. The gel images and histograms shown in Figure 3 and Table 3 provide a quantitative analysis of the oxidative DNA damage induced by a whole-particle suspension and a water-soluble fraction in five particle doses (25, 50, 100, 300, 500 μg ml^{-1}). It can be seen that with increasing doses, the particle-induced DNA damage for all of the coal burning-derived PM_{10} types showed a general increasing trend. A positive dose-response relationship exists between the amounts of DNA damages and the sample doses, which implies that higher mass concentrations of PM in the ambient air could cause a higher oxidative potential, and thus a higher toxicity per cubic metre of air.

The amount of damage to the plasmid DNA that was induced by coal burning-derived PM_{10} varied from 5% to 55%. Table 3 and Figure 3 also demonstrated that, under the same dose (Table 3), the oxidative potential of both the whole-particle suspension and the water-soluble fraction of the PM_{10} followed a clear pattern. High from the ZJ and DT honeycomb briquettes emissions, moderately high from the YC and ZJ powdered coals emissions, and relatively low from the DT, DS, and JX powdered coals and wood charcoal emissions.

It was found that the oxidative potential of the PM_{10} generated from burning honeycomb briquettes was significantly higher than that generated by burning the corresponding raw powdered coals. At a particle dose of 500 μg ml^{-1}, the PM_{10} generated from burning ZJ and DT honeycomb briquettes induced DNA damage of 55% and 46% by their whole-particle suspension respectively, which was higher than the damage percentages of 34% and 19% from their corresponding raw powdered coals.

Furthermore, the differences between the amount of DNA damage induced by the whole-particle suspension and the corresponding water-soluble fraction of the PM_{10} samples at all dose levels were relatively small. Figure 4 shows a comparison between the amount of DNA

damage resulting from the whole-particle suspension and from the soluble fraction of the coal burning-derived PM_{10} at a dose of 500 μg ml^{-1}; it is clear that the differences between the amount of DNA damage induced by the whole-particle suspension and by the corresponding water-soluble fraction of these PM_{10} were mostly insignificant, ranging from 4% to 30%, but mostly less than 20%. The amount of damage induced by the soluble fraction can contribute more than 70% to the amount of damage induced by the whole-particle suspension. This result indicates that the oxidative potential of the PM_{10} generated by coal burning-derived is mainly sourced from their water-soluble components.

3.3 Trace elements in the PM_{10} emitted by burning different coals

An ICP-MS was used to detect the concentration of elements in the coal burning-derived PM_{10}. The elements analysed included As, Cd, Co, Cr, Cs, Cu, Ge, Mo, Mn, Ni, Pb, Sb, Se, Sr, Ti, Tl, V, and Zn. The concentrations of these elements in their water-soluble fractions were analysed and the results were reported in weight ppm of each element in its soluble state in the original intact PM_{10} samples (Table 4).

For the total analysed water-soluble elements, the PM_{10} emitted by burning the ZJ honeycomb briquette had the highest level (21480.63 ppm), followed by those emitted by burning the DT honeycomb briquette (5658.73 ppm). For coal samples the values were YC powdered coal (3960.71 ppm), the ZJ powdered coal (3196.05 ppm), the DT powdered coal (219.28 ppm), the DS powdered coal (212.65 ppm), the JX powdered coal (201.52 ppm), and the wood charcoal (140.11 ppm) in descending order. It is clear that the PM_{10} particles emitted by burning honeycomb briquettes produced a higher content of total analysed water-soluble trace elements than those emitted by burning raw powdered coals, with the lowest values being the PM_{10} emitted by burning wood charcoal.

Table 4 also showed that the PM_{10} emitted by burning honeycomb briquettes was enriched with water-soluble elements such as As, Cd, Cu, Ge, Mn, Ni, Pb, Se, Sb, Ti, Tl, V, and Zn. All of these elements were present at concentrations greater than 10 ppm, and the water-soluble As, Ge, Pb, Tl, and Zn were present at levels greater than 100 ppm. For the raw powdered coals, the coal burning-derived PM_{10} was enriched with water-soluble As, Cu, Ni, Pb, Ti, and Zn; these individual elements reached levels that were greater than 10 ppm.

4 Discussion

4.1 Relationship between the oxidative potential and the content of water-soluble trace elements

To examine the most probable source of the oxidative potential of the coal burning PM_{10}, the amounts of DNA damage were correlated with corresponding concentrations of the water-soluble elements in the intact PM_{10} samples. As the DNA damage values from all particle doses showed the same trend, we only choose one dose level (500 μg ml^{-1}) for the correlation analysis. The Pearson correlation coefficients are provided in Table 5, with a sample number n=8 and a threshold correlation coefficient of 0.71 at 95% confidence level.

The particle-induced oxidative potential displayed a significant positive correlation with the total analysed water-soluble metal concentrations with a Pearson correlation coefficient of 0.87, implying that the oxidative potential of coal burning-derived PM_{10}s was derived mainly from its water-soluble elements. This finding was also supported by the fact that the whole-particle suspension of these coal burning-derived PM_{10} induced similar amounts of DNA damages relative to their corresponding water-soluble fractions.

The correlation coefficients between the particle-induced oxidative potentials from a dosage of 500 μg ml^{-1} and the concentrations of individual water-soluble heavy metals in PM (Table 5) can be used to determine which individual elements were most responsible for the particle-induced oxidative potential of these coal burning-derived PM_{10}. The water-soluble As, Cd, Ge, Mn, Ni, Pb, Sb, Se, Tl, and Zn exhibited relatively significant positive correlations with the oxidative potential (correlation coefficients higher than 0.71), indicating that these elements in their water-soluble states were likely responsible for the plasmid DNA damage. Similar conclusions have been reached by other reports for PM_{10}, from Beijing (Shao et al., 2006, Sun et al., 2014) and in the UK (Moreno et al., 2004; Merolla and Richards, 2005; Reche et al., 2012).

Some previous studies (Querol et al., 2006; Liu et al., 2010) have shown that heavy metal pollutants, such as Cr, Zn, Pb, and Mn, can be produced from combustion-related industry. Tang and Huang (2004) and Ren et al.(2006) found that high levels of As, Se, Zn and Pb might

be sourced from the combustion of different types of coal, and all of these elements are considered to be potentially harmful to human health. The results of this study demonstrated the occurrence of Cr and Zn, and to a lesser extent Pb and Mn in coal burning-derived PM_{10}; although this does depend on the geochemistry of the original coal.

4.2 Possible causes of the variation in the oxidative potential of coal burning-derived PM_{10}.

The PM_{10} emitted by burning honeycomb briquettes had a higher content of total analysed water-soluble trace elements and a higher oxidative potential than those emitted by burning raw powdered coals. This can be attributed to the clay mixed into the briquettes, which would enrich the inorganic elements in the PM_{10}, effectively being released as fly ash.

For the intact powdered coals, the variations in the oxidative potential could be explained by the raw coal quality; especially in terms of the difference in the sulphur and ash content. The higher percentages of total water-soluble trace elements and the higher oxidative potential of the PM_{10} emitted by burning ZJ powdered coal can be attributed to the higher sulphur content of the raw ZJ coal (Table 1). The sulphur-rich coals of the Late Permian age from the Zhijin coal mining area of southwestern China normally contain higher levels of pyritic sulphur that tends to be associated with some toxic heavy metals (Ren et al., 2006). Therefore, the PM_{10} emitted by burning high-sulphur coal would have higher percentages of trace elements and a higher oxidative potential.

The PM_{10} that was emitted by burning YC powdered coal also had higher percentages of total water-soluble trace elements and a higher oxidative potential. This could have been because the YC powdered coal had a higher ash content (Table 1). The high coal ash content tends to be accompanied by higher levels of certain trace elements (Ren et al., 2006). This finding allows us to infer that the PM_{10} emitted by burning high-ash coals can be associated with a relatively high percentage of water-soluble trace elements, thereby inducing a high oxidative potential. The JX coal had high ash content but was associated with a lower PM_{10}-induced oxidative potential. This is due to the lower sulphur content in the raw coal.

4.3 Exposure risk of the PM_{10} emitted by burning different coal types

In order to elucidate the exposure risk to humans we devised a toxicity index to represent

the relative risk for people exposed to the ambient air with different types of coal burning-derived PM_{10}:

$$TI = MC \times P_{DNA}$$

In this formula, *TI* represents toxicity index, *MC* represents the mass concentration of the coal burning-derived PM_{10}, P_{DNA} represented the percentage of DNA damage at the 500 μg/ml PM_{10} dose. Table 6 showed that the *TI* of the PM_{10} emitted by burning YC raw powdered coal and DS raw powdered coal were much higher than that by burning other types of coals. It can also been seen that the *TI* values of the PM_{10} emitted by burning ZJ and DT honeycomb briquettes, (70987 and 31754 respectively) were clearly lower than those by burning their corresponding raw powdered coals (96577 and 80265 respectively). This result indicated that exposure to the PM_{10} emitted by burning raw powdered coals is associated with higher risks to human health than exposure to the PM_{10} emitted by burning honeycomb briquettes.

5. Conclusion

1) Burning raw powdered coal emits more PM_{10} than burning honeycomb briquette. The oxidative potential of the PM_{10} emitted by burning honeycomb briquettes was significantly higher than that by burning raw powdered coals and wood charcoal.

2) The PM_{10} emitted by burning honeycomb briquettes had a higher content of total water-soluble trace elements than that emitted by burning raw powdered coals and wood charcoal. The PM_{10} particles emitted by burning honeycomb briquettes were enriched with water-soluble As, Ge, Pb, Tl, and Zn, and the PM_{10} particles emitted by burning raw powdered coals was enriched with water-soluble As, Cu, Ni, Pb, Ti, and Zn.

3) The oxidative potential of the coal burning-derived PM_{10} was mainly sourced from their water-soluble fractions. The water-soluble As, Cd, Ge, Mn, Ni, Pb, Sb, Se, Tl, and Zn showed the most significant correlation with the oxidative potential, implying that these elements in their water-soluble states were responsible for the particle-induced DNA damage.

4) The PM_{10} emitted by burning coals with high levels of mixed clay, sulphur, and ash is associated with a correspondingly high percentage of water-soluble trace elements, thereby

inducing a high oxidative potential.

5) The exposure risk to humans from the PM_{10} emitted by burning raw powdered coal was significantly higher than that from burning honeycomb briquette emissions.

Acknowledgements

This work was supported by the National Basic Research Program of China (Grant No. 2013CB228503) and the National Natural Science Foundation of China (Grant No. 41175109). Two anonymous reviewers are thanked for their helpful comments.

References

Adamson I Y R, Prieditis H, Hedgecock C. Vincent R. Zinc is the toxic factor in the lung response to an atmospheric particulate sample. Toxicology and Applied Pharmacology 2000; 166: 111–119.

Andreae M O, Merlet P. Emission of trace gases and aerosols from biomass burning. Global Biogeochemical Cycles 2001; 15: 955-966.

Benbrahim-Tallaa, L., Baan, R.A., Grosse, Y., Lauby-Secretan, B., Ghissassi, F.E., Bouvard, V., Guha, N., Loomis, D., Straifa, K.. Carcinogenicity of diesel-engine and gasoline-engine exhausts and some nitroarenes. The Lancet Oncology 2012; 13: 663-664.

Bogdanovic I, Fazinic S, Itskos S, et al.. Trace element characterization of coal fly ash particle. Nuclear Instrument and Methods in Physics Research B 1995; 99: 402-405.

Geng, C., Wang, K., Wang, W., Chen, J., Liu, X., Liu, H.. Smog chamber study on the evolution of fume from residential coal combustion. Journal of Environmental Sciences 2012; 24: 169-176.

Chen Y Q, Liu H. The analysis of toxic trace elements in coal and fly ash in the region of Beijing. Comprehensive Utilization Of Fly Ash 2009; 3: 20-22.

China Statistic Department. China Statistics Yearbook 2013.

Chuang H C, Jones T, Lung S C, BéruBé K A. Soot-driven reactive oxygen species formation from incense burning. Science of Total Environment 2011; 409: 4781-4787.

Chuang H C, BéruBé K A, Lung S C, Bai K J, Jones T. Investigation into the oxidative potential generated by the formation of particulate matter from incense combustion. Journal of Hazardous Materials 2013; 244-245: 142-150.

Costa D L, Dreher K L. Bioavailable transition metals in particulate matter mediate cardiopulmonary injury in healthy and compromised animal models. Environmental Health Perspectives 1997; 105: 1053–1060.

Crabbe H. Risk of respiratory and cardiovascular hospitalization with exposure to bushfire particulates: new evidence from Darwin, Australia. Environmental Geochemistry and Health 2012; 34: 697-709.

Dockery D W, Pope III A, Xu X, Spengler J D, Ware J H, Fay M E, Ferris B G, Jr., Speizer F E. An association between air-pollution and mortality in 6 United-States cities. The New England Journal of Medicine 1993; 329: 1753-1759.

Dai S F, Ren D Y, Liu J R, Li S S. The occurrence and distribution of toxic trace elements in the coal of Fengfeng mine of Hebei Province. Journal of China University of mining and technology 2003; 32(4):

358-361.
Distefano E, Eiguren-Fernandez A, Delfino R J, Sioutas C, Froines J R, Cho A K. Determination of metal-based hydroxyl radical generating capacity of ambient and diesel exhaust particles. Inhalation Toxicology 2009; 21: 731-738.
Donaldson K, Beswick P H, Gilmour P S. Free radical activity associated with the surface of the particles: a unifying factor in determining biological activity. Toxicology Letters 1996; 88: 293-298.
Greenwell L L, Moreno T, Richard R J. Pulmonary antioxidants exert differential protective effects against urban and industrial particulate matter. Journal of Biosciences 2003; 28: 101–107.
Hoek G, Krishnan RM, Beelen R, Peters A, Ostro B, Brunekreef B, Kaufman J D. Long-term air pollution exposure and cardio-respiratory mortality: a review. Environmental Health 2013; 12: 43.
Jones T, Wlodarczyk A, Koshy L, Brown P, Shao L Y, BéruBé K. The geochemistry and bioreactivity of fly-ash from coal-burning power stations. Biomarkers 2009; 14(S1): 45–48.
Kan H, London S, Chen G, ZhangY, Song G, Zhao N, Jiang L, Chen B. Differentiating the effects of fine and coarse particles on daily mortality in Shanghai, China. Environment International 2007; 33: 376–384.
Kan H, Chen R, Tong S. Ambient air pollution, climate change, and population health in China. Environment International 2012; 42: 10–19.
Kheirbek I, Wheeler K, Walters S, Kass D, Matte T. $PM_{2.5}$ and ozone health impacts and disparities in New York City: sensitivity to spatial and temporal resolution. Air Quality, Atmosphere and Health 2013; 6: 473-486.
Lan Q, Mumford J L, Shen M, Demarini D M, Bonner M R, He X, Yeager M, Welch R, Chanock S, Tian L, Chapman R S, Zheng T, Keohavong P, Caporaso N, Rothman N. Oxidative damage-related genes AKR1C3 and OGG1 modulate risks for lung cancer due to exposure to PAH-rich coal combustion emissions. Carcinogenesis 2004; 25(11): 2177-2181.
Levine J S, Cofer W R, Cahoon D R, Winstead E L. Biomass burning: a driver for global change. Environmental Science & Technology 1995; 29: 120A-125A.
Luo W Q. Briefly on the atmospheric pollution and its control by burning coals. Energy saving technology 2008; 26: 267-268.
Li S S. Problems and countermeasures of the harmful trace elements in Chinese coal. Coal science and technology 2006; 34(1): 28-31.
Li X Y, Gilmour P S, Donaldson K, MacNee W. In vivo and in vitro proin- flammatory effects of particulate air pollution (PM_{10}). Environmental Health Perspectives 1997; 105: 1279–1283.
Lin Z Q, Xi Z G, Chao F H. Research progress in the toxicity effects of the nano particles. Journal of Preventive Medicine of Chinese People's Liberation Army 2007; 25: 383–386.
Liu Y W, Mao X L, Sun L Y, Ni J R. Characteristics of heavy metals discharge from industrial pollution sources in Shenzhen. Acta Scientiarum Naturalium Universitatis Pekinensis 2010; 46: 279-285.
Loomis D, Grosse Y, Lauby-Secretan B, Ghissassi F E, Bouvard V, Benbrahim-Tallaa L, Guha N, Baan R, Mattock H, Straif K. The carcinogenicity of outdoor air pollution, Lancet Oncology 2013; 14:1262-1263.
Lu S L, Shao L Y, Wu M H, Jones, T P, Merolla L, Richard, R J. The related research of the bioactivity and trace elements of PM_{10} in Beijing. Science in China D: Geochemistry 2006; 36(8): 777-784.
Merolla L, Richards R J. In vitro effects of water-soluble metals present in UK particulate matter. Experimental Lung Research 2005; 31: 671–683.
Moreno T, Merolla L, Gibbons W, Greenwell L, Jones T, Richards R. Variations in the source, metal content and bioreactivity of technogenic aerosols: a case study from Port Talbot, Wales, UK. Science of Total

Environment 2004; 333: 59–73.
Neas L M. Fine particulate matter and cardiovascular disease. Fuel Processing Technology 2000; 65-66: 55-67.
Ostro B, Broadwin R, Green S, Feng W Y, Lipsett M. Fine particulate air pollution and mortality in nine California counties: Result from CALFINE. Environmental Health Perspectives 2006; 114(1): 29-33.
Pui D Y H, Chen S C, Zuo Z. $PM_{2.5}$ in China: Measurements, sources, visibility and health effects, and mitigation. Particuology 2014; 13: 1-26.
Querol X, Zhuang X, Alastuey A, Viana M, Lv W, Wang Y, Lopez A , Zhu Z, Wei H, Xu S. Speciation and sources of atmospheric aerosols in a highly industrialised emerging mega-city in Central China. Journal of Environmental Monitoring 2006; 8: 1049-1059.
Ren D Y, Zhao F H, Dai S F, et al. The Trace Element Geochemistry of Coal, Beijing: Science Press; 2006.
Reche C, Moreno T, Amato F, Viana M, van Drooge B L, Chuang H C, et al.. A multidisciplinary approach to characterise exposure risk and toxicological effects of PM_{10} and $PM_{2.5}$ samples in urban environments. Ecotoxicology and Environmental Safety 2012; 78: 327-335.
Samet J M, Dominici F, Curreiro F C, Coursac I, Zeger S L. Fine particulate air pollution and mortality in 20 US cities, 1987-1994. The New England Journal of Medicine 2000; 343: 1742-1749.
Sánchez-Pérez Y, Chirino Y I, Osornio-Vargas A R, Morales-Bárcenas R, Gutiérrez-Ruíz C, Vázquez-López I, et al.. DNA damage response of A549 cells treated with particulate matter (PM_{10}) of urban air pollutants. Cancer Letters 2009; 278(2): 192-200.
See S W, Wang Y H, Balasubramanian R. Contrasting reactive oxygen species and transition metal concentrations in combustion aerosols. Environmental Research 2007; 103: 317-324.
Shao L Y, Hu Y, Wang J, Hou C, Yang Y Y, Wu M Y. Particle-induced oxidative damage of indoor PM_{10} from coal burning homes in the lung cancer area of Xuan Wei, China. Atmospheric Environment 2013; 77: 959-967.
Shao L Y, Jones T P, Gayer R A, Dai S F, Li S S, Jiang Y F. Petrology and geochemistry of the high-sulphur coals from the Upper Permian carbonate coal measures in the Heshan Coalfield, southern China. International Journal of Coal Geology 2003; 55: 1-26.
Shao L Y, Li J J, Zhao H Y, Yang S S, Li H, Li W J, Jones T P, Sexton K, BéruBé K A. Associations between particle physicochemical characteristics and oxidative capacity: an indoor PM_{10} study in Beijing, China. Atmospheric Environment 2007; 41: 5316–5326.
Shao L Y, Shi Z B, Jones T P, Li J J, Whittaker A G, BéruBé K A. Bioreactivity of particulate matter in Beijing air: results from plasmid DNA assay. Science of The Total Environment 2006; 367: 261-272.
Straif K, Baan R, Grosse Y, Secretan B, El Ghissassi F, Cogliano V. Carcinogenicity of household solid fuel combustion and of high-temperature frying. The Lancet Oncology 2006; 7: 977-978.
Sun Z Q, Shao L Y, Mu Y J, Hu Y. Oxidative capacities of size-segregated haze particles in a residential area of Beijing. Journal of Environmental Sciences 2012; 26: 167–174.
Tang X Y, Huang W H. Trace elements in coal in China, Beijing: The commercial press; 2004.
Vidrio E, Phuah CH, Dillner A M, Anastasio C. Generation of hydroxyl radicals from ambient fine particles in a surrogate lung fluid solution. Environmental Science & Technology 2009; 43: 922-927.
Wang J, Shao L Y, Geng C M, Wang J Y, Liu J X, Yang W, Hu Y. Oxidative capacity of PM_{10} emitted by burning coals. Journal of Central South University (Science and Technology) 2014; 45(6): 2137-2143 (in Chinese)
Whittaker A G. Black smokes: Past and present. The Thesis for the Degree of Ph.D. Cardiff University, 2003.
Xiao Z H, Shao L Y, Zhang N, Wang J, Wang J Y. Heavy metal compositions and bioreactivity of airborne

PM_{10} in a valley-shaped city in northwestern China. Aerosol and Air Quality Research 2013; 13: 1116–1125.

Xu M H, Yan R, Zheng C G, Qiao Y, Han J, Sheng C D. Status of trace element emission in a coal combustion process: a review. Fuel Processing Technology 2003; 85: 215-237.

Zhang W L, Xu D Q, Cui J S. Air pollutant $PM_{2.5}$ monitoring and study on its genotoxicity. Journal of Environment and Health 2003; 1: 3–4.

Zhong C Y, Zhou Y M, Smith K R, Kennedy I M, Chen C Y, Aust A E, Pinkerton K E. Oxidative injury in the lungs of neonatal rats following short-term exposure to ultrafine iron and soot particles. Journal of Toxicology and Environmental Health, Part A: Current Issues 2010; 73: 837-847.

Tables:

Table 1. Information of the proximate and ultimate analysis of the raw coals used in this study

Table 2. Mass concentration of the PM_{10} emitted by burning different coals ($\mu g/m^3$)

Table 3. Percentage of DNA damage induced by the PM_{10} emitted from burning different fuels

Table 4. Contents of water-soluble trace elements in the intact whole PM_{10} emitted from burning different types of coal and wood charcoal (ppm)

Table 5. Correlation coefficients between the total and individual water-soluble heavy metal concentrations and the percentages of DNA damage by coal-burning PM_{10}

Table 6. Toxic index of the PM_{10} emitted by burning different coals

Figures:

Fig.1 Sketch diagram showing composition of the coal combustion stove system which contains a stove, a dilution tunnel and the smoke chambers. “HC” represents honeycomb briquette; “RC” represents raw powdered coal.

Fig.2 A comparison between the morphology and the quantity of PM_{10} emitted by burning honeycomb briquette and raw powdered coal. DT-H and ZJ-H represent Datong and Zhijin honeycomb briquettes respectively, DT-R and ZJ-R represent Datong and Zhijin raw powdered coals respectively.

Fig.3 Gel images and histograms of the oxidative damage on DNA that was induced by PM_{10} emitted by burning different fuels. (“a” represents ZJ honeycomb briquette; “b” represents DT honeycomb briquette; “c” represents ZJ powder coal; “d” represents DT powder coal; “e” represents DS powder coal; “f” represents YC powder coal; “g” represents JX powder coal; “h” represents wood charcoal; “W” represents the whole-particle suspension; and “S” represents the water soluble fraction).

Fig. 4. Comparison between the DNA damage percentages of the whole particles and the water-soluble fraction of the coal burning-derived PM_{10} under a dose of $500 mg ml^{-1}$ (“H” represents honeycomb briquette, “R” represents raw powdered coal).

570 Table 1. Information of the proximate and ultimate analysis of the raw coals used in this study

	Proximate analysis						Ultimate analysis				
	moisture %	ash content %	Volatiles %	Fixed carbon %	Higher heating value MJ/kg	Lower heating value MJ/kg	S%	C%	H%	N%	O%
Coal of ZJ	0.94	9.08	5.76	84.22	31.82	31.23	2.24	81.86	2.76	1.04	2.08
Coal of DT	6.98	9.50	32.07	51.45	27.12	26.19	0.21	64.6	3.56	0.84	14.31
Coal of DS	7.46	6.68	30.82	55.04	28.45	27.51	0.20	68.72	3.76	0.90	12.28
Coal of YC	1.30	23.28	19.74	55.68	19.85	19.51	0.36	62.68	2.16	0.62	9.60
Coal of JX	3.02	26.34	4.44	66.20	22.96	22.73	0.25	68.26	0.79	0.26	1.08

571 Note: the above content is for the air dry basis of coal; “ZJ” represents Zhijin; “DT” represents Datong; “DS” represents
572 Dongsheng; “YC” represents Yinchuan; and “JX” represents Jingxi.
573

574 Table 2 Mass concentration of the PM_{10} emitted by burning different coals (μg /m^3)

Fuel types	Mass (μg)	flow rate (L/min)	sampling time (min.)	mass concentration (μg/m^3)
ZJ-H	7800	78	78	1282.05
DT-H	4300	78	80	689.10
ZJ-R	13400	78	60	2863.25
DT-R	18100	78	56	4143.77
DS-R	34200	78	41	10694.18
YC-R	16100	78	29	7117.60
JX-R	5600	78	50	1435.90

575 Note: H represents honeycomb briquettes; R represents raw powdered coal.

576

577

578 Table 3. Percentages of DNA damage induced by the PM_{10} emitted from burning different fuels

Fuel Types	Samples status	Dosage of PM_{10}(μg/ml)				
		25	50	100	300	500
ZJ-H	Whole-particle suspension (%)	12.46(±0.69)	30.70(±1.67)	33.03(±1.48)	38.61(±2.49)	55.37(±1.91)
	Water-soluble fraction (%)	14.05(±0.02)	23.42(±1.05)	25.89(±0.75)	36.73(±0.89)	48.34(±1.40)
DT-H	Whole-particle suspension (%)	12.29(±1.14)	11.95(±1.75)	26.22(±0.22)	37.85(±1.18)	46.08(±1.34)
	Water-soluble fraction (%)	10.98(±0.94)	11.35(±2.09)	22.54(±0.38)	34.10(±1.58)	44.97(±1.70)
ZJ-R	Whole-particle suspension (%)	13.32(±0.36)	15.18(±0.39)	17.17(±1.11)	23.18(±1.43)	33.73(±1.22)
	Water-soluble fraction (%)	8.58(±0.37)	9.63(±0.71)	11.79(±1.39)	23.81(±0.30)	23.61(±0.98)
DT-R	Whole-particle suspension (%)	12.55(±0.24)	13.59(±0.18)	13.44(±0.60)	20.09(±0.64)	19.37(±0.15)
	Water-soluble fraction (%)	7.70(±0.46)	9.86(±0.04)	9.30(±0.16)	12.37(±0.37)	15.60(±0.92)
DS-R	Whole-particle suspension (%)	10.33(±0.65)	11.29(±0.25)	12.24(±0.06)	14.27(±0.18)	16.85(±0.45)
	Water-soluble fraction (%)	7.58(±0.06)	10.14(±0.86)	12.46(±0.91)	13.57(±0.04)	15.52(±0.13)
YC-R	Whole-particle suspension (%)	15.68(±1.85)	16.62(±0.27)	20.70(±0.45)	31.89(±0.74)	33.70(±1.14)
	Water-soluble fraction (%)	20.66(±1.26)	22.51(±0.79)	23.02(±0.28)	25.52(±0.43)	30.01(±1.49)
JX-R	Whole-particle suspension (%)	6.83(±0.81)	8.84(±0.79)	11.65(±0.67)	14.71(±0.83)	16.37(±0.50)
	Water-soluble fraction (%)	4.84(±0.74)	7.45(±0.26)	8.85(±1.38)	10.72(±0.83)	12.21(±1.11)
wood charcoal	Whole-particle suspension (%)	11.37(±0.93)	12.25(±0.07)	14.48(±0.69)	15.55(±0.13)	16.99(±1.05)
	Water-soluble fraction (%)	11.61(±1.01)	11.89(±0.75)	13.15(±0.20)	13.95(±1.42)	14.38(±0.25)

579 Note: “H” represents honeycomb briquettes, “R” represents raw powdered coal, “±” represent error range

580

581 Table 4. Contents of water-soluble trace elements in the intact whole PM_{10} emitted from burning different types of coal and
582 wood charcoal (ppm)

	ZJ-H	DT-H	ZJ-R	DT-R	DS-R	YC-R	JX-R	Wood charcoal
As	412	155	19.6	19.9	18.3	46.5	9.46	19.7
Cd	93.6	15.8	10.3	0.08	0.23	19.8	0.6	0.3
Cr	1.92	9.08	9.36	8.02	3.09	5.2	3.99	13.5
Co	0.6	1.92	0.15	0.63	1	0.23	0.02	—
Cs	2.57	6.42	2.97	4.48	2.3	5.9	3.88	5.34
Cu	86.4	16.2	278	12.4	8.69	18.8	15.3	16.5
Ge	890	37.5	7.88	2.86	2.71	1.08	0.471	0.74
Mn	16.6	30.5	12.2	0.42	1.44	8.76	3.79	—
Mo	13	5.02	3.73	7.36	7.57	7.5	2.56	2
Ni	47.4	22.7	22.9	13.6	19	8.37	18.8	13.1
Pb	2385	824	324	0.39	2.12	77.1	3.39	16
Se	61.3	43.2	10.5	12	2.57	4.16	1.5	8.88
Sr	8.28	7.86	12.3	3.15	2.23	10.1	5.42	14
Sb	46.5	14.8	0.93	1.92	9.38	4.21	1.16	0.75
Ti	84.1	19.5	61.5	29.2	65.2	20.5	56.6	3.16
Tl	179	98.1	9.86	2.76	1.73	16.5	2.19	4.83
V	2.36	1.13	1.87	1.9	1.59	4	1.39	2.5
Zn	17150	4350	2408	98.2	63.5	3702	71	18.8
Total	21480.63	5658.73	3196.05	219.28	212.65	3960.71	201.52	140.11

583 Note: "—"represents that the measured values of the corresponding element are below the detection limit. "Total" represents
584 sum of the analysed elements. "H" represents honeycomb briquettes. "R" represents raw powdered coal.
585

586 Table 5. Correlation coefficients between the total and individual water-soluble heavy metal concentrations and the
587 percentages of DNA damage by coal-burning PM_{10}

Elements	As	Cd	Cr	Co	Cs	Cu	Ge	Mn	Mo	Ni
DNA damage percentages at 500 μg/ml	0.854	0.828	-0.237	0.335	0.047	0.305	0.712	0.823	0.595	0.718
Elements	Pb	Se	Sb	Sr	Ti	Tl	V	Zn	total	
DNA damage percentages at 500 μg/ml	0.869	0.882	0.785	0.258	0.284	0.898	0.111	0.871	0.870	

588

589 Table 6. Toxic index of the PM_{10} emitted by burning different coals

Fuel types	mass concentration ($\mu g/m^3$)	percentage of DNA damage at 500 μg/ml dose	toxicity index
ZJ-H	1282.05	55.37	70987
DT-H	689.10	46.08	31754
ZJ-R	2863.25	33.73	96577
DT-R	4143.77	19.37	80265
DS-R	10694.18	16.85	180197
YC-R	7117.60	33.70	239863
JX-R	1435.90	16.37	23506

590 Note: “H” represents honeycomb briquette, “R” represents raw powdered coal.

591

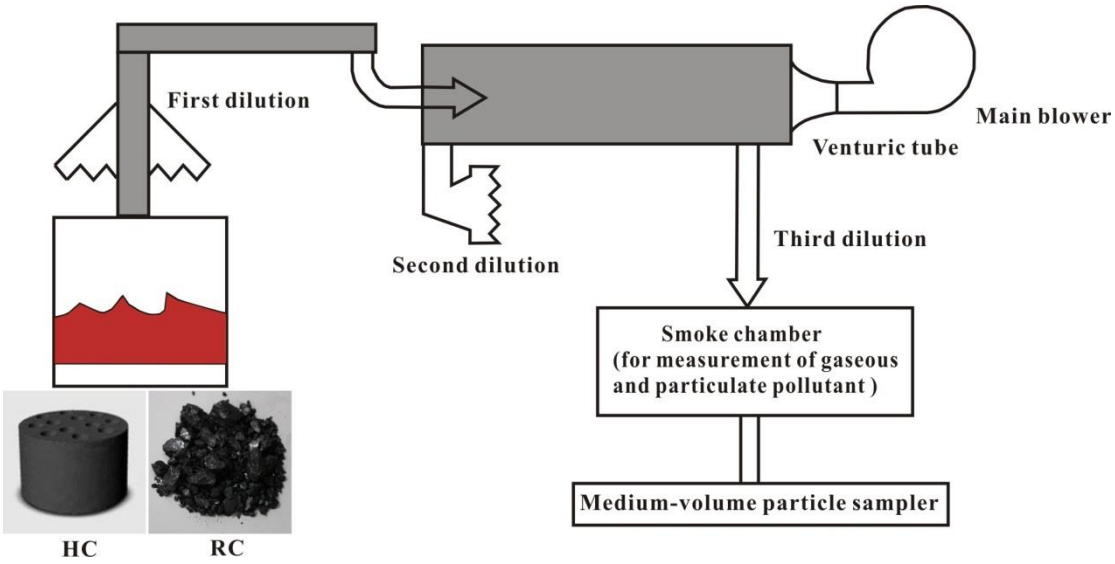

Fig.1 Sketch diagram showing composition of the coal combustion stove systems which contains a stove, a dilution tunnel and the smoke chambers. “HC” represents honeycomb briquette; “RC” represents raw powdered coal

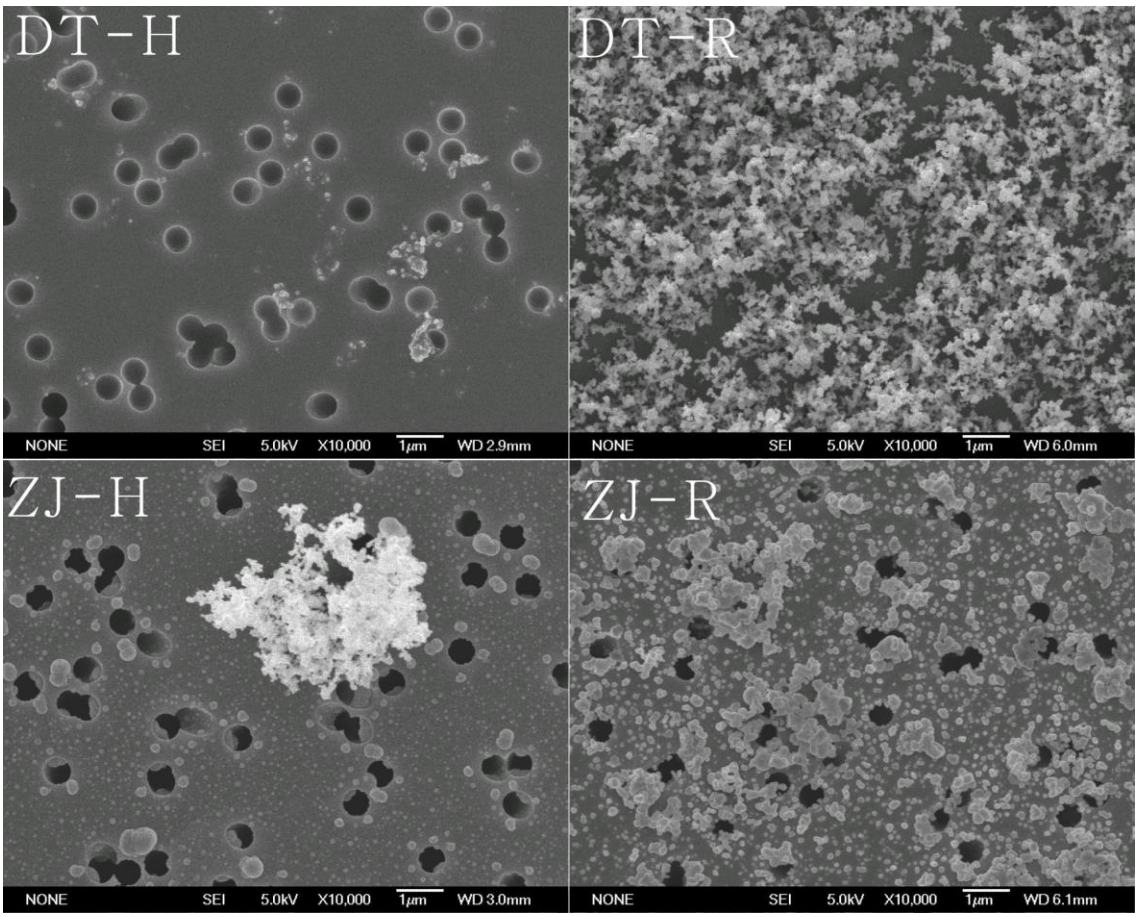

Fig.2 A comparison between the morphology and the quantity of PM_{10} emitted by burning honeycomb briquette and raw powdered coal. DT-H and ZJ-H represent Datong and Zhijin honeycomb briquettes respectively, DT-R and ZJ-R represent Datong and Zhijin raw powdered coals respectively.

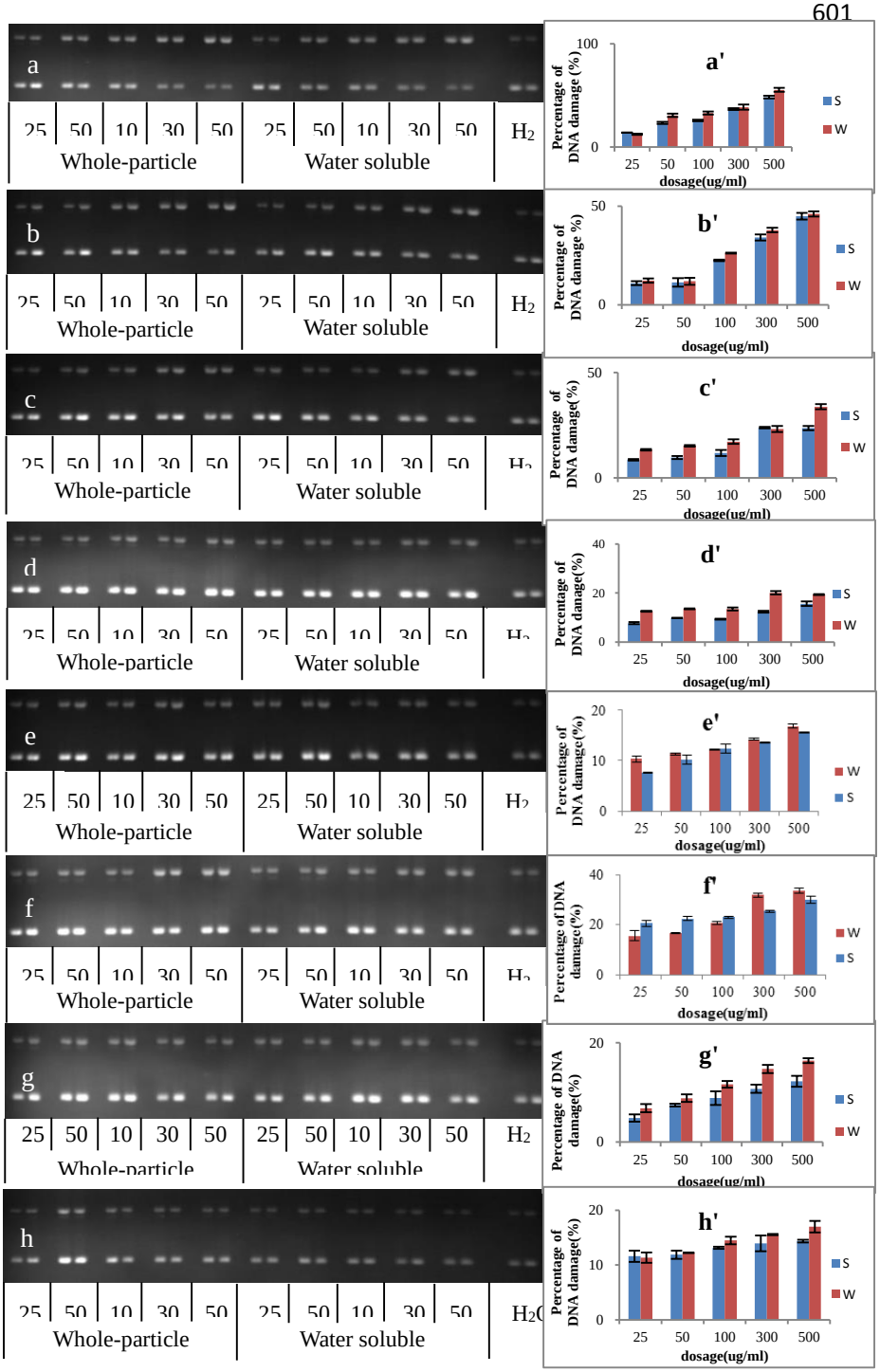

Fig.3 Gel images and histograms of the oxidative damage on DNA that was induced by PM_{10} emitted by burning different fuels. ("a" represents ZJ honeycomb briquette; "b" represents DT honeycomb briquette; "c" represents ZJ powder coal; "d" represents DT powder coal; "e" represents DS powder coal; "f" represents YC powder coal; "g" represents JX powder coal; "h" represents wood charcoal; "W" represents the whole-particle suspension; and "S" represents the water soluble fraction).

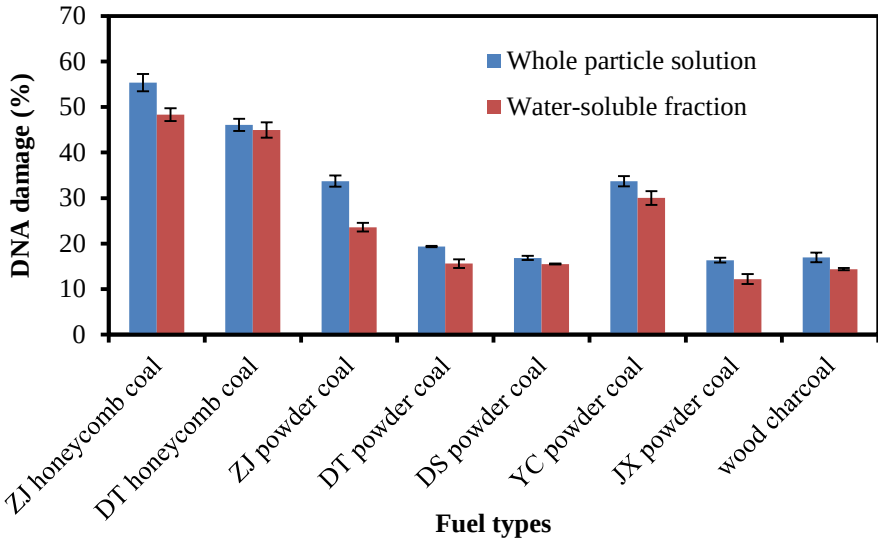

627

628 Fig. 4. Comparison between the DNA damage percentages of the whole particles and the water-soluble fraction of the coal

629 burning-derived PM_{10} under a dose of 500mgml^{-1}.